Mechanics Research Communications 38 (2011) 449–455

Contents lists available at ScienceDirect

Mechanics Research Communications

journal homepage: www.elsevier.com/locate/mechrescom

Heat conduction and thermal analysis in multilayered plates and shells

S. Brischetto[a,*], E. Carrera[b]

[a] Department of Aeronautics and Space Engineering, Politecnico di Torino, Corso Duca degli Abruzzi, 24, 10129 Torino, Italy
[b] Professor of Aerospace Structures and Computational Aeroelasticity, Department of Aeronautics and Space Engineering, Politecnico di Torino, Italy

ARTICLE INFO

Article history:
Received 4 April 2011
Available online 12 June 2011

Keywords:
Assumed temperature profile
Calculated temperature profile
Fourier heat conduction equation
Multilayered plates and shells.

ABSTRACT

This work solves the Fourier heat conduction equation in the case of layered structures embedding orthotropic layers in order to obtain a calculated temperature profile in the thickness direction. The calculated temperature profile $\theta(z)$ is obtained for both plate and shell geometries. Several comparisons between the calculated temperature profile and the usual assumption of linear form of $\theta(z)$ in the thickness direction are given. A wrong temperature profile gives an erroneous thermal load for the static analysis of layered structures. Proposed results show the effect of a wrong use of $\theta(z)$ on the static response of multilayered plates and shells. It is concluded that in the analysis of multilayered structures the correct solution of the heat conduction equation could be mandatory with respect to any further evaluation.

1. Introduction

The effects of both high-temperature and mechanical loadings have to be considered in the design process of typical aeronautical structures, such as one-layered isotropic and multilayered composite plates and shells. An accurate description of local stress fields, related to temperature variations in the layers, is mandatory to prevent thermally loaded structure failure mechanisms (Noor and Burton, 1992). These structures are subjected to severe thermal environments, such as high temperatures, high gradients and cyclic changes in temperature; typical examples are the thin-walled members of reactor vessels, turbines, the structures of future supersonic and hypersonic vehicles, such as high-speed civil transport and advanced tactical fighters (Thornton, 1996).

Computational models, developed to study the behavior of high-temperature one-layered and composite plates and shells, make use of partially coupled thermo-mechanical analysis. This means that the temperature is only considered as an external load and the temperature profile must be a priori defined: considering it linear through the thickness direction or calculating it by solving the Fourier heat conduction equation. In each developed computational model, the stress analysis should be preceded by an accurate thermal analysis, which provides the temperature input data required for the thermal external load (Carrera, 2002). A satisfactory thermal stress analysis is only possible if advanced and refined computational models are developed to correctly approximate the stiffness matrix, and if a correct thermal load is recognized. Sometimes the evaluation of a correct thermal load could be mandatory with respect to any further evaluation for the computational models. In this paper, the authors desire to demonstrate as the assumption of "a priori" linear temperature profile in the thickness direction could be wrong for particular shell and plate configurations, and as the use of the Fourier heat conduction equation could result mandatory to obtain a correct thermal load. Therefore, we would like to demonstrate as a wrong thermal load invalidates the static response of plate and shell structures even when advanced computational models are employed.

In the open literature a large amount of works have discussed the thermal stress analysis, but the present paper should give a general overview of the problem by means of few simple and suggestive examples. Some computational models where the temperature was considered "a priori" linear through the thickness direction are listed as follows. Wu and Chen (2008) have investigated displacements and stresses in laminated structures under thermal bending assuming a linear temperature profile through the thickness direction. In Brischetto and Carrera (2009), the same linear temperature profile has been used to asses the accuracy of several refined models for the static analysis of multilayered composite shells. The deflection of composite laminates and laminated or sandwich shells has been evaluated by means of a linear temperature profile through the thickness direction by Bhaskar et al. (1996) and Khare et al. (2003). Khdeir (1996) has solved the thermoelastic governing equations by assuming a linear or constant temperature profile through the thickness. An interesting method to analyze the thermal stresses in shells is the use of Cosserat surfaces, as done by Birsan (2009) for two given temperature fields. Other computational models have used a calculated temperature profile because in the case of multilayered anisotropic

* Corresponding author. Tel.: +39 011 564 6813; fax: +39 011 564 6899.
E-mail address: salvatore.brischetto@polito.it (S. Brischetto).

0093-6413/$ – see front matter © 2011 Elsevier Ltd. All rights reserved.
doi:10.1016/j.mechrescom.2011.05.016

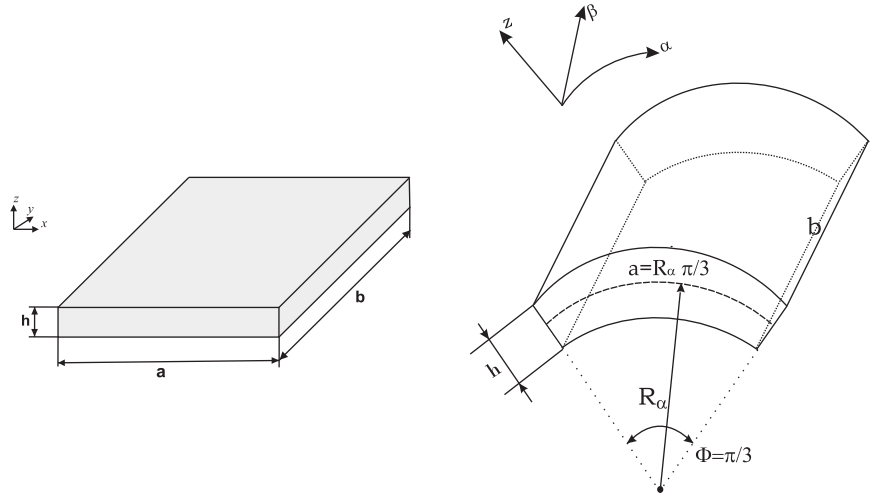

Fig. 1. Geometry and reference system of the considered plates and cylindrical shell panels.

structures, the temperature profile is never linear, even when the plate or shell is thin: an incorrect temperature profile gives an erroneous thermal load which leads to larger errors, even though the structural model is accurate (Carrera, 2000, 2002). A finite element shell has been developed by Rolfes et al. (1999) to analyze composite structures simultaneously loaded by mechanical and thermal loads; the temperature profile has been presumed linear or quadratic in the thickness direction and then introduced into the Fourier heat conduction equation. The Fourier heat conduction equation has been solved by the authors for multilayered composite shells and for functionally graded material plates in Brischetto (2009) and Brischetto et al. (2008), respectively. The calculated temperature profile gives an appropriate thermal load to correctly investigate the thermal deflection of such structures. In the previous authors' works, the Fourier heat conduction equation has been solved in according to the technique presented by Tungikar and Rao (1994).

2. Heat conduction problem in layered structures

The heat conduction problem is investigated by solving the Fourier heat conduction equation as described in Tungikar and Rao (1994) for the plate case. Here the solution is given for the shell case as proposed in Brischetto (2009), the plate geometry can be considered as a particular case of the shell geometry when the radii of curvature are infinite. The proposed shell is supposed simply supported, the curvilinear reference system (α, β, z) and the geometrical data are given in Fig. 1, a and b are the shell dimensions and h is the thickness value.

If the values of the temperature are known at the top and bottom surface of the shell, the temperature profile through the thickness can be considered in two different ways. The first method introduces an assumed profile $\hat{\theta}(z)$ that varies linearly from the top to the bottom; the second one computes $\hat{\theta}(z)$ by solving the Fourier heat conduction equation. The temperature is assumed bi-sinusoidal in the plane (α, β) at the top and bottom shell surfaces:

$$\theta(\alpha, \beta, z) = \hat{\theta}(z) \sin\left(\frac{m\pi}{a}\alpha\right) \sin\left(\frac{n\pi}{b}\beta\right) \tag{1}$$

with amplitudes $\hat{\theta}(+h/2) = \hat{\theta}_{top} = +1.0$ and $\hat{\theta}(-h/2) = \hat{\theta}_{bot} = 0.0$. θ indicates the sovra-temperature value considered with respect to the external room temperature. m and n are the wave numbers. In the case of assumed temperature profile (θ_a) a linear through the thickness distribution is considered from +1.0 to 0.0. Independently by the number of considered layers the linear profile is always the same. The temperature profile is approximated in the thickness direction by means of the Carrera Unified Formulation (CUF) (Carrera, 1995, 2003) as:

$$\theta^k(\alpha, \beta, z) = F_\tau(z)\theta^k_\tau(\alpha, \beta) \qquad \text{with } \tau = t, b, r \text{ and } r = 2, \ldots, 4, \tag{2}$$

t and b indicate the top and bottom of the considered kth layer. The thickness functions F_τ are a combination of Legendre polynomials, for further details see Carrera (1995, 2003). If the temperature is assumed linear through the thickness, the values at the top and bottom surface, and therefore F_t and F_b, would be sufficient to describe the assumed profile via CUF. The calculation procedure for the actual temperature in case of one or more layers is reported in the following in order to obtain the values of θ^k_τ for Eq. (2).

If the considered shell is subjected to a bi-sinusoidal thermal load at the top and the bottom, the thermal boundary conditions are:

$$\theta = 0 \quad \text{at } \alpha = 0, a \text{ and } \beta = 0, b; \quad \hat{\theta}(-h/2) = \hat{\theta}_{bot}\,; \quad \hat{\theta}(h/2) = \hat{\theta}_{top}, \tag{3}$$

where m and n are the wave numbers along the two in-plane shell directions (α, β). a and b are the shell dimensions, h is the shell thickness, and $\hat{\theta}_{bot}$ and $\hat{\theta}_{top}$ are the amplitudes of the temperature at the bottom and top, respectively.

In case of multi-layered structures, continuity conditions for the temperature θ and the transverse normal heat flux q_z hold in the thickness direction at each kth layer interface, reading:

$$\theta^k_t = \theta^{k+1}_b, \qquad q^k_{zt} = q^{k+1}_{zb} \quad \text{for } k = 1, \ldots, N_l - 1, \tag{4}$$

where N_l is the number of layers in the considered structure. The relationship between the transverse heat flux and the temperature is given as:

$$q^k_z = K^k_3 \frac{\partial \theta^k}{\partial z}\,. \tag{5}$$

In general for the kth homogeneous orthotropic layer, the differential Fourier equation of heat conduction reads:

$$\left(\frac{K^k_1}{H^{k\,2}_\alpha}\right)\frac{\partial^2\theta}{\partial\alpha^2} + \left(\frac{K^k_2}{H^{k\,2}_\beta}\right)\frac{\partial^2\theta}{\partial\beta^2} + K^k_3\frac{\partial^2\theta}{\partial z^2} = 0. \tag{6}$$

K^k_1, K^k_2 and K^k_3 are the thermal conductivities along the three shell directions α, β and z, that are constant in each layer. ∂ indicates the partial derivative. $H^k_\alpha = (1 + z^k/R^k_\alpha)$, $H^k_\beta = (1 + z^k/R^k_\beta)$ and $H^k_z = 1$ are the metric coefficients which describe the shell geometry (for

details see Leissa, 1973). In case of plates (see Fig. 1), Eq. (6) can be easily solved because $H_\alpha^k = H_\beta^k = 1$ and the coefficients K_1^k, K_2^k and K_3^k are constant for each layer k. In case of shell we can define three new coefficients $K_1^{*k} = K_1^k/{H_\alpha^k}^2$, $K_2^{*k} = K_2^k/{H_\beta^k}^2$ and $K_3^{*k} = K_3^k$, which in a generic layer k depend on the thickness coordinate of the shell, so:

$$K_1^{*k}\frac{\partial^2\theta}{\partial\alpha^2} + K_2^{*k}\frac{\partial^2\theta}{\partial\beta^2} + K_3^{*k}\frac{\partial^2\theta}{\partial z^2} = 0. \tag{7}$$

Eq. (7) has not constant coefficients in the layer k. It can be solved by introducing for each layer k a given number of mathematical layers (N_{ml}). Considering with N_l the number of physical layers, a new index j can be defined which goes from 1 to $(N_l \times N_{ml})$. So the continuity of temperature and transverse heat flux can be written in each jth mathematical interface:

$$\theta_t^j = \theta_b^{j+1}, \qquad q_{zt}^j = q_{zb}^{j+1} \quad \text{for } j = 1, \ldots, (N_l \times N_{ml} - 1) \tag{8}$$

where

$$q_z^j = K_3^j\frac{\partial\theta^j}{\partial z}. \tag{9}$$

Eq. (7) can be rewritten for each mathematical layer j:

$$K_1^{*j}\frac{\partial^2\theta}{\partial\alpha^2} + K_2^{*j}\frac{\partial^2\theta}{\partial\beta^2} + K_3^{*j}\frac{\partial^2\theta}{\partial z^2} = 0. \tag{10}$$

In these mathematical layers we can suppose K_1^{*j} and K_2^{*j} constant because in each mathematical layer we can calculate the values of H_α^j and H_β^j. For a mathematical layer, both governing equations and boundary conditions are satisfied by assuming the following temperature field:

$$\theta(\alpha, \beta, z) = f(z)\sin\left(\frac{m\pi\alpha}{a}\right)\sin\left(\frac{n\pi\beta}{b}\right) \tag{11}$$

with

$$f(z) = \theta_0\,\exp\left(s^j z\right), \tag{12}$$

θ_0 is a constant and s^j a parameter. Substituting Eq. (11) in Eq. (10) and solving for s^j:

$$s_{1,2}^j = \pm\sqrt{\frac{K_1^{*j}(m\pi/a)^2 + K_2^{*j}(n\pi/b)^2}{K_3^{*j}}}. \tag{13}$$

Therefore

$$f(z) = \theta_{01}^j\,\exp(s_1^j z) + \theta_{02}^j\,\exp(s_1^j z) \quad \text{or}$$
$$f(z) = C_1^j\,\cosh(s_1^j z) + C_2^j\,\sinh(s_1^j z). \tag{14}$$

The solution for a mathematical layer j can be written as:

$$\theta_c(\alpha, \beta, z) = \theta^j = [C_1^j\,\cosh(s_1^j z) + C_2^j\,\sinh(s_1^j z)]\sin\left(\frac{m\pi\alpha}{a}\right)\sin\left(\frac{n\pi\beta}{b}\right) \tag{15}$$

wherein the coefficients C_1^j and C_2^j are constant for each mathematical layer j.

In Eq. (14) for each mathematical layer j two unknowns (C_1^j and C_2^j) remain. Therefore, if the number of layers is N_l, the number of mathematical layers are $N_l \times N_{ml}$, the number of unknowns is $2N_l \times N_{ml}$ and we need $2N_l \times N_{ml}$ equations to determine the unknowns. As we know the temperature at the top and the bottom surface, we have already two conditions:

$$\begin{aligned}\hat\theta_{bot} &= C_1^1\,\cosh(s_1^1 z_{bot}) + C_2^1\,\sinh(s_1^1 z_{bot}),\\ \hat\theta_{top} &= C_1^{N_l\times N_{ml}}\,\cosh(s_1^{N_l\times N_{ml}} z_{top}) + C_2^{N_l\times N_{ml}}\,\sinh(s_1^{N_l\times N_{ml}} z_{top}).\end{aligned} \tag{16}$$

Another $(N_l \times N_{ml} - 1)$ equations can be obtained from the continuity of temperature at each mathematical interface, and finally $(N_l \times N_{ml} - 1)$ equations result from the continuity of the heat flux through the interfaces, compare Eq. (8). Thus, we have:

$$\begin{aligned}&C_1^j\,\cosh(s_1^j z_t^j) + C_2^j\,\sinh(s_1^j z_t^j) - C_1^{j+1}\,\cosh(s_1^{j+1} z_b^{j+1}) - C_2^{j+1}\,\sinh(s_1^{j+1} z_b^{j+1}) = 0,\\ &s_1^j K_3^j[C_1^j\,\cosh(s_1^j z_t^j) + C_2^j\,\sinh(s_1^j z_t^j)] - s_1^{j+1}K_3^{j+1}[C_1^{j+1}\,\cosh(s_1^{j+1} z_b^{j+1}) - C_2^{j+1}\,\sinh(s_1^{j+1} z_b^{j+1})] = 0.\end{aligned} \tag{17}$$

In Eqs. (16) and (17), z_{top} and z_{bot} indicate the coordinates of top and bottom of the whole shell. z_t^j and z_b^{j+1} represent the top of the jth mathematical layer and the bottom of the $(j+1)$th mathematical layer, respectively.

Solving the system given by Eqs. (16) and (17), we gain the $2N_l \times N_{ml}$ coefficients C_1^j and C_2^j. The actual temperature amplitude in the thickness shell direction is then given by:

$$\hat\theta_c(z) = \hat\theta^j = C_1^j\,\cosh(s_1^j z) + C_2^j\,\sinh(s_1^j z) \quad \text{with } j = 1, \ldots, (N_l \times N_{ml}). \tag{18}$$

We compute the temperature at different values z_N of the thickness coordinate. By solving the system in Eq. (19), we obtain the N values of θ_τ^k for the CUF:

$$\begin{bmatrix}\hat\theta_c(z_1)\\ \hat\theta_c(z_2)\\ \vdots\\ \hat\theta_c(z_N)\end{bmatrix} = \begin{bmatrix}F_0(z_1) & F_1(z_1) & \cdots & F_N(z_1)\\ F_0(z_2) & F_1(z_2) & \cdots & F_N(z_2)\\ \vdots & \vdots & \vdots & \vdots\\ F_0(z_N) & F_1(z_N) & \cdots & F_N(z_N)\end{bmatrix}\begin{bmatrix}\theta_0^k\\ \theta_1^k\\ \vdots\\ \vdots\\ \theta_N^k\end{bmatrix}. \tag{19}$$

So, if we consider a generic multilayered shell, the temperature profile is approximated by Eq. (2) and the N values of θ_τ^k are given by Eq. (19). In Eq. (19) $\hat\theta_c$ is calculated by means of the mathematical layers j in certain points that permit the correspondence with the physical layers k. For the plate geometry (see Fig. 1) the procedure is simpler because the coefficients K_1^k, K_2^k and K_3^k are constant in the layer (there is not the effect of the curvature) and there is not the necessity to introduce the mathematical layers: the procedure described above can be repeated directly by using the physical layers k (details can be found in Carrera (2002)).

3. Numerical results and discussion

The investigated one-layered and multilayered shells and plates are considered simply supported with an harmonic distribution of the temperature as described in Eq. (1). The imposed wave numbers in α and β directions are $m = 1$ and $n = 1$, respectively. The geometry of the considered shells and plates is given in Fig. 1. The square plate has in-plane dimensions $a = b = 1$ m and total thickness $h = 0.2$ m and $h = 0.02$ m for thick and thin plates, respectively. This means investigated thickness ratios a/h equal 5 and 50. The shell panel has radius of curvature R_α in α direction equals 10 m and infinite radius of curvature R_β in β direction. The in-plane dimensions are $a = (\pi/3)R_\alpha = 10.47197551$ m and $b = 1$ m, the total thickness is $h = 1.0$ m and $h = 0.01$ m for thickness ratios $R_\alpha/h = 10$ and $R_\alpha/h = 1000$, respectively. The imposed sovra-temperatures at the top and bottom surfaces are $\hat\theta(+h/2) = \hat\theta_{top} = +1.0$ and

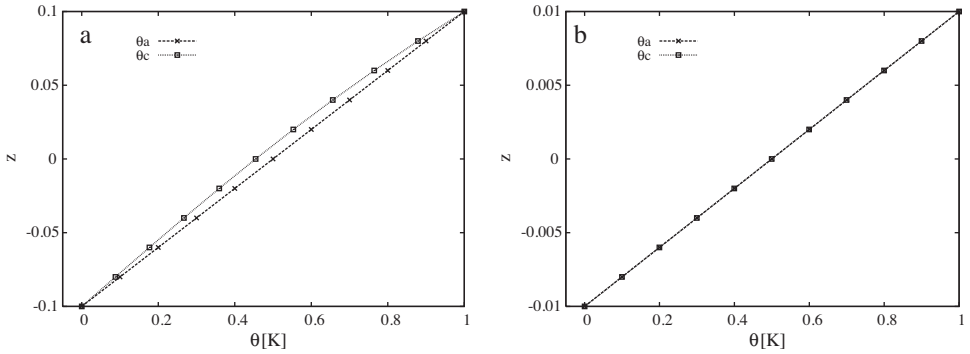

Fig. 2. One-layered isotropic plate in Al5086, assumed (θ_a) vs. calculated (θ_c) temperature profile in the thickness direction for thickness ratios $a/h = 5$ (a) and $a/h = 50$ (b).

$\hat{\theta}(-h/2) = \hat{\theta}_{bot} = 0.0$, respectively. For several layered structures a comparison is made between the assumed linear temperature profile (θ_a) and the calculated temperature profile (θ_c) as described in Section 2. The differences between the θ_a and θ_c cases give different evaluations of the thermal load, this fact is clearly demonstrated by the static response given in terms of transverse displacements $\bar{w}$.

The considered layered configurations are seven. The first one is a one-layered isotropic structure in Al5086 with Young modulus $E = 70.3$ GPa, Poisson ratio $\nu = 0.33$, thermal expansion coefficient $\mu = 24 \times 10^{-6}$ 1/K and conductivity coefficient $K = 130$ W/mK. The second configuration is a one-layered orthotropic structure in Graphite-Epoxy with longitudinal Young modulus $E_1 = 172.72$ GPa and transverse Young modulus $E_2 = E_3 = 6.909$ GPa. Poisson ratio is $\nu_{12} = \nu_{13} = \nu_{23} = 0.25$ and shear modulus is $G_{12} = G_{13} = 3.45$ GPa and $G_{23} = 1.38$ GPa. Longitudinal and transverse thermal expansion coefficients are $\mu_1 = 0.57 \times 10^{-6}$ 1/K and $\mu_2 = \mu_3 = 35.6 \times 10^{-6}$ 1/K, respectively. Longitudinal conductivity coefficient is $K_1 = 36.42$ W/mK and transverse conductivity coefficients are $K_2 = K_3 = 0.96$ W/mK. The third case is a two-layered isotropic structure with the bottom layer in Al5086 ($h_1 = 0.5$ h) and the top layer in Ti22 ($h_2 = 0.5$ h). The elastic and thermal properties of the Ti22 layer are $E = 110$ GPa, $\nu = 0.32$, $\mu = 8.6 \times 10^{-6}$ 1/K and $K = 21.9$ W/mK. The fourth case considers a two-layered composite structure embedding two Graphite-Epoxy layers of the same thickness ($h_1 = h_2 = 0.5$ h) and lamination sequence $0^\circ/90^\circ$. A three-layered isotropic structure is considered as fifth case, the bottom layer is in Al5086, the middle layer is in Ti22 and the top layer is in Al2024. The three layers have the same thickness $h_1 = h_2 = h_3 = (1/3)$ h and the elastic and thermal properties of the Al2024 layer are $E = 73$ GPa, $\nu = 0.3$, $\mu = 25 \times 10^{-6}$ 1/K and $K = 130$ W/mK. The case number six considers a sandwich structure with faces in Al5086 (thickness of each face $h_1 = h_3 = 0.1$ h) and core in PVC with thickness $h_2 = 0.8$ h. The elastic and thermal properties of the PVC core are $E = 3$ GPa, $\nu = 0.4$, $\mu = 50 \times 10^{-6}$ 1/K and $K = 0.18$ W/mK. The last case is a sandwich structure with core in PVC and faces made of a two-layered Graphite-Epoxy part with fiber orientation $0^\circ/90^\circ$, therefore the global lamination sequence is $0^\circ/90^\circ/core/90^\circ/0^\circ$. The thickness of the PVC core is $h_3 = 0.6$ h and the thickness of each Graphite-Epoxy layer is $h_1 = h_2 = h_4 = h_5 = 0.1$ h.

3.1. Evaluation of the temperature profile

The temperature profiles in the thickness direction are given for the proposed seven layered structures in Figs. 2–8 for both plate and shell geometries because the introduction of the curvature does not give any further considerations. In each figure, a comparison is made between the linear assumed temperature profile (θ_a) and the calculated temperature profile by means of the Fourier heat conduction equation (θ_c) for both cases of thick and moderately thin plates and shells. Fig. 2 considers the one-layered isotropic plate in Al5086, the temperature profile in the thickness direction is linear for thin structures and the calculated temperature profile coincides with the assumed one. For thick plate, even if the plate is one-layered and isotropic, the actual temperature profile is not linear and a difference exists between the (θ_a) and (θ_c) case. The same considerations can be made for the orthotropic one-layered plate considered in Fig. 3, in this case a larger difference is remarked for the thick case: the solution of the Fourier heat conduction equation is sensitive for the longitudinal conductivity coefficient K_1 that is different from the transverse ones $K_2 = K_3$. When the structure has two different isotropic layers as in Fig. 4 for the shell case, even if it is thin, the temperature profile is linear in each layer but with different slopes (effect due to the different conductivity coefficients, for the Al5086 and the Ti22 layers, in Eqs. (8) and (9) written for the continuity of the transverse heat flux at the interfaces). In the two-layered orthotropic shell of Fig. 5 the temperature profile is

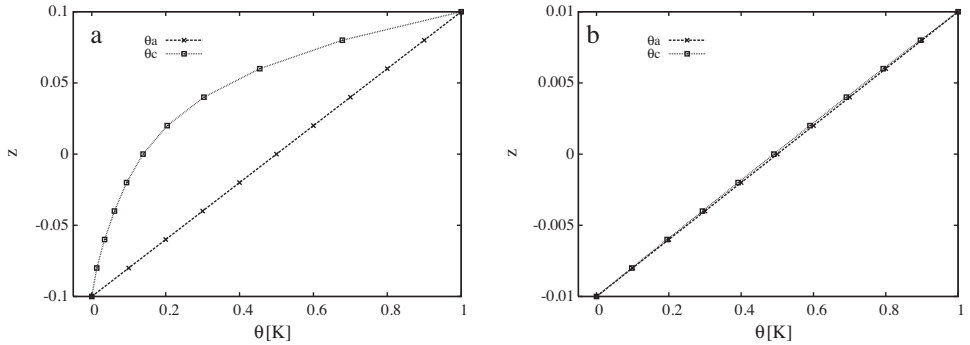

Fig. 3. One-layered orthotropic plate in Graphite-Epoxy, assumed (θ_a) vs. calculated (θ_c) temperature profile in the thickness direction for thickness ratios $a/h = 5$ (a) and $a/h = 50$ (b).

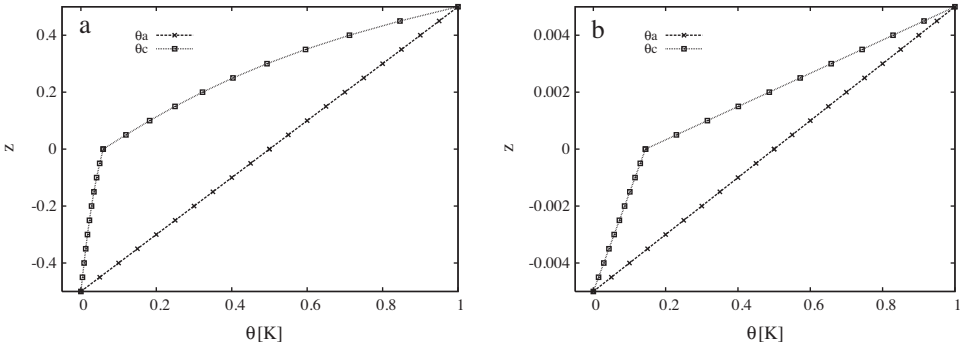

Fig. 4. Two-layered isotropic shell in Al5086 (bottom layer) and Ti22 (top layer), assumed (θ_a) vs. calculated (θ_c) temperature profile in the thickness direction for thickness ratios $R_\alpha/h = 10$ (a) and $R_\alpha/h = 1000$ (b).

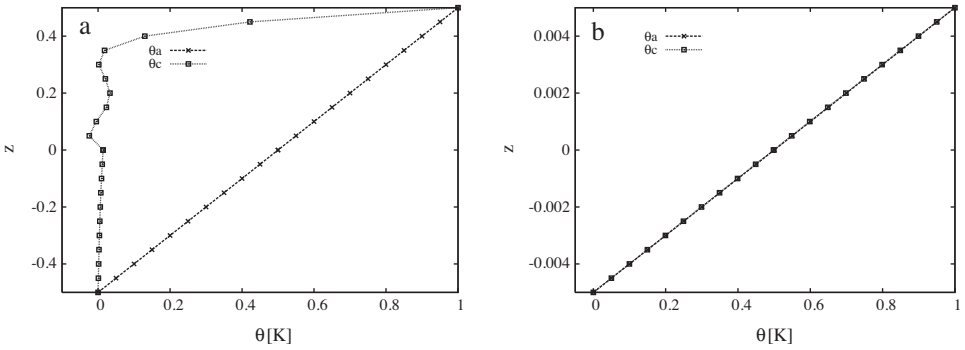

Fig. 5. Two-layered orthotropic shell in Graphite-Epoxy ($0^\circ/90^\circ$), assumed (θ_a) vs. calculated (θ_c) temperature profile in the thickness direction for thickness ratios $R_\alpha/h = 10$ (a) and $R_\alpha/h = 1000$ (b).

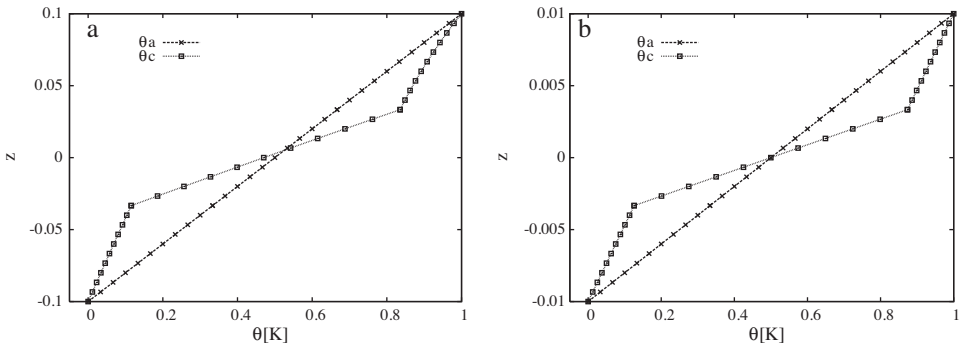

Fig. 6. Three-layered isotropic plate in Al5086 (bottom layer), Ti22 (middle layer) and Al2024 (top layer), assumed (θ_a) vs. calculated (θ_c) temperature profile in the thickness direction for thickness ratios $a/h = 5$ (a) and $a/h = 50$ (b).

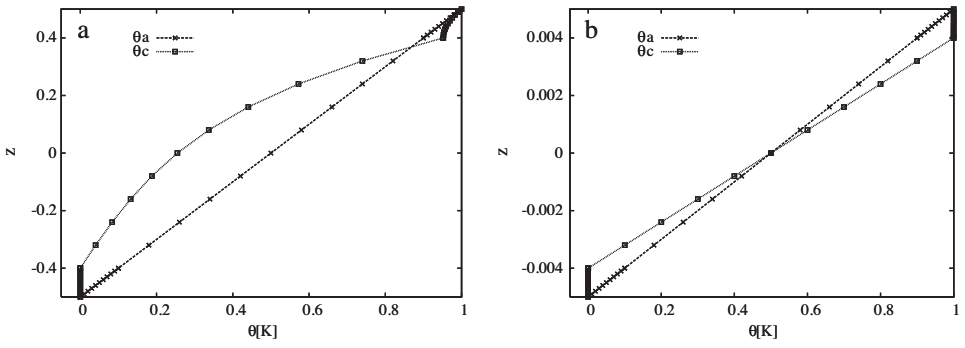

Fig. 7. Sandwich shell with faces in Al5086 and core in PVC, assumed (θ_a) vs. calculated (θ_c) temperature profile in the thickness direction for thickness ratios $R_\alpha/h = 10$ (a) and $R_\alpha/h = 1000$ (b).

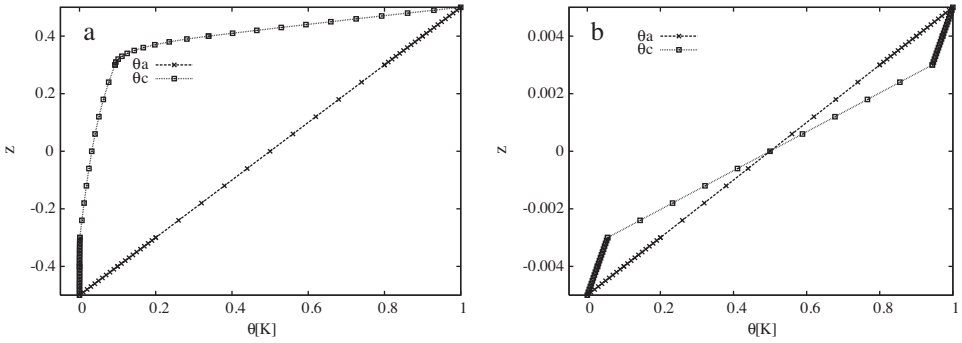

Fig. 8. Sandwich shell with faces in Graphite-Epoxy and core in PVC, assumed (θ_a) vs. calculated (θ_c) temperature profile in the thickness direction for thickness ratios $R_\alpha/h = 10$ (a) and $R_\alpha/h = 1000$ (b).

Table 1
Transverse displacement $\bar{w} = (10\, w\, h/a^2\, \mu\, \Delta T)$ for the one-layered isotropic plate in Al5086 and $\bar{w} = (10\, w\, h/a^2\, \mu_2\, \Delta T)$ for the one-layered orthotropic plate in Graphite-Epoxy. Assumed (θ_a) vs. calculated (θ_c) temperature profile.

a/h	5	50	5	50
	Al5086		Graphite Epoxy	
$\bar{w}(h/2), \theta_a$	0.8598	0.6756	0.2501	0.0609
$\bar{w}(h/2), \theta_c$	0.8503(1.12%)	0.6756(0.00%)	0.2191(14.1%)	0.0608(0.16%)
$\bar{w}(0), \theta_a$	0.6603	0.6736	0.0824	0.0592
$\bar{w}(0), \theta_c$	0.6521(1.26%)	0.6736(0.00%)	0.0705(16.9%)	0.0591(0.17%)
$\bar{w}(-h/2), \theta_a$	0.5940	0.6730	0.0335	0.0587
$\bar{w}(-h/2), \theta_c$	0.5848(1.57%)	0.6729(0.01%)	0.0133(>100%)	0.0586(0.17%)

Table 2
Transverse displacement $\bar{w} = (10\, w\, h/b^2\, \mu_{Al5086}\, \Delta T)$ for the two-layered isotropic shell in Al5086 (bottom layer) and Ti22 (top layer) and $\bar{w} = (10\, w\, h/b^2\, \mu_2\, \Delta T)$ for the two-layered orthotropic shell in Graphite-Epoxy ($0^\circ/90^\circ$). Assumed (θ_a) vs. calculated (θ_c) temperature profile.

R_α/h	10	1000	10	1000
	Al5086–Ti22		Graphite Epoxy	
$\bar{w}(h/2), \theta_a$	2.0130	0.2629	3.1659	0.0312
$\bar{w}(h/2), \theta_c$	1.6500(22.0%)	0.1773(48.3%)	1.7592(80%)	0.0312(0.00%)
$\bar{w}(0), \theta_a$	0.4668	0.2627	−1.0080	0.0307
$\bar{w}(0), \theta_c$	0.4153(12.4%)	0.1772(48.2%)	−0.4709(>100%)	0.0307(0.00%)
$\bar{w}(-h/2), \theta_a$	−1.0471	0.2626	−1.9824	0.0306
$\bar{w}(-h/2), \theta_c$	0.1952(>100%)	0.1772(48.2%)	−0.3786(>100%)	0.0306(0.00%)

linear in the case of thin structure because even if the two layers have different fiber orientation, the transverse conductivity coefficient K_3 is the same and in the two layers the temperature profile has the same slope. When a three-layered plate with three different isotropic layers are considered, as in Fig. 6, the temperature profile is never linear even when the plate is thin. There are three different linear temperature profiles in each layer with different slopes: Al5086, Ti22 and Al2024 layers have three different conductivity coefficients (see the analogy with the case of the two-layered isotropic shell considered in Fig. 4). Sandwich configurations are investigated in Figs. 7 and 8 for the case of isotropic faces and Graphite-Epoxy layers: the same considerations already given for the other multilayered plates and shells are here confirmed, each layer has a different conductivity coefficient and this fact means temperature profile linear for each layer when the shell is thin, but with different slopes. The proposed cases clarify the importance of a calculated temperature profile for the cases of thick plates/shells and/or for the case of multilayered configurations with transverse anisotropy in terms of thermal and mechanical properties.

3.2. Effect on the static response

The temperature profiles obtained in Section 3.1, permit to calculate the thermal load for the static response investigation. The governing equation is:

$$\boldsymbol{K}_{uu}\, \boldsymbol{u} = -\boldsymbol{K}_{u\theta}\theta, \tag{20}$$

where the thermal load is $\boldsymbol{p}_\theta = -\boldsymbol{K}_{u\theta}\,\theta$, and $\boldsymbol{K}_{uu}$ is the global stiffness matrix written for the displacement vector $\boldsymbol{u}$. The displacement is approximated in the thickness direction, by means of CUF (Carrera, 1995, 2003); for each layer k is possible to write:

$$\boldsymbol{u}^k(\alpha, \beta, z) = F_0(z)\boldsymbol{u}_0^k(\alpha, \beta) + F_1(z)\boldsymbol{u}_1^k(\alpha, \beta) + F_2(z)\boldsymbol{u}_2^k(\alpha, \beta) + F_3(z)\boldsymbol{u}_3^k(\alpha, \beta) + F_4(z)\boldsymbol{u}_4^k(\alpha, \beta), \tag{21}$$

the thickness functions $F_\tau(z)$ are combination of Legendre polynomial (see Carrera, 1995, 2003) and this permits to consider $\boldsymbol{u}_0^k$ as the displacement at the top of each layer k and $\boldsymbol{u}_1^k$ as the displacement at the bottom of each layer k, the other values are the higher orders of expansion. The vector $\boldsymbol{u}^k(\alpha, \beta, z)$ contains the three displacements components u, v and w for each layer k. It is possible to

Table 3
Transverse displacement $\bar{w} = (10\, w\, h/a^2\, \mu_{Al5086}\, \Delta T)$ for the three-layered isotropic plate in Al5086 (bottom layer), Ti22 (middle layer) and Al2024 (top layer). Assumed (θ_a) vs. calculated (θ_c) temperature profile.

a/h	5	50
$\bar{w}(h/2), \theta_a$	0.8284	0.6670
$\bar{w}(h/2), \theta_c$	0.9971(16.9%)	0.8373(20.3%)
$\bar{w}(0), \theta_a$	0.6570	0.6653
$\bar{w}(0), \theta_c$	0.8064(18.5%)	0.8353(20.3%)
$\bar{w}(-h/2), \theta_a$	0.6082	0.6648
$\bar{w}(-h/2), \theta_c$	0.7828(22.3%)	0.8351(20.4%)

Table 4
Transverse displacement $\bar{w} = (10\, w\, h/b^2\, \mu_{Al5086}\, \Delta T)$ for the sandwich shell with faces in Al5086 and core in PVC and $\bar{w} = (10\, w\, h/a^2\, \mu_2\, \Delta T)$ for the sandwich shell with faces in Graphite-Epoxy and core in PVC. Assumed (θ_a) vs. calculated (θ_c) temperature profile.

R_α/h	10	1000	10	1000
	Faces in Al5086		Faces in Graphite Epoxy	
$\bar{w}(h/2), \theta_a$	10.163	0.7317	6.3613	0.0872
$\bar{w}(h/2), \theta_c$	9.8627(3.04%)	0.7604(3.77%)	1.9084(>100%)	0.0903(3.43%)
$\bar{w}(0), \theta_a$	0.3593	0.7306	−0.3497	0.0864
$\bar{w}(0), \theta_c$	0.3191(12.6%)	0.7592(3.77%)	0.2088(>100%)	0.0893(3.25%)
$\bar{w}(-h/2), \theta_a$	−2.3113	0.7303	−2.5131	0.0860
$\bar{w}(-h/2), \theta_c$	−1.7885(29.2%)	0.7591(3.79%)	0.0152(>100%)	0.0891(3.48%)

write the same expansion for the sovra-temperature $\theta^k(\alpha, \beta, z)$:

$$\theta^k(\alpha, \beta, z) = F_0(z)\theta_0^k(\alpha, \beta) + F_1(z)\theta_1^k(\alpha, \beta) + F_2(z)\theta_2^k(\alpha, \beta) + F_3(z)\theta_3^k(\alpha, \beta) + F_4(z)\theta_4^k(\alpha, \beta)\,. \tag{22}$$

When a linear temperature profile is imposed, it is sufficient to know the values at the top and bottom of each layer k (θ_0^k and θ_1^k). In the case of calculated temperature profile, the values for the Eq. (22) are obtained from the solution of the Eq. (19).

By means of the above governing equation, it is possible to consider a refined model for the mechanical part, for both cases of assumed (θ_a) and calculated (θ_c) temperature profile. In this way the effect in terms of static response can be evaluated. Details about the matrices $\boldsymbol{K}_{uu}$ and $\boldsymbol{K}_{u\theta}$ can be found in Brischetto (2009) and Carrera (2002), where the Carrera Unified formulation is detailed. The no-dimensional transverse displacement $\bar{w} = (10\, w\, h/a\, \mu\, \Delta T)$ (with $\Delta T = 1$ K) is evaluated at the top, middle and bottom of each proposed structure when a linear temperature profile is assumed or an actual temperature profile is calculated. Either cases of thin and thick plates/shells are considered. Tables 1–4 consider the proposed seven layered plates and shells. In each table is clear that when the temperature profile is approximated in a wrong way, the thermal load is not correct and this fact gives large errors even if the displacement components are approximated in a very refined way. The differences in percentage between the displacement obtained with the assumed temperature profile and that obtained with the calculated temperature profile ($\Delta(\%) = |(\bar{w}(\theta_a) - \bar{w}(\theta_c))/\bar{w}(\theta_c)| \times 100$) are put in brackets in each considered table. The largest errors are obtained for the cases of thick multilayered transverse anisotropic plates and shells. In some cases, even if the plate or shell is thin, the error is large because the assumption of linear temperature profile is completely wrong.

4. Conclusions

In this work the Fourier heat conduction equation has been solved for one-layered and multilayered plates and shells in order to obtain the actual temperature profile. Comparisons have been made with the assumption of linear temperature profile in the thickness direction. It is concluded that the assumption of linear temperature profile is wrong when the structure is thick or moderately thick, and the error remains for thin plates and shells when the structure is multilayered. A correct evaluation of the temperature profile is mandatory to calculate the opportune thermal load which permits a satisfactory static thermo-mechanical response.

References

Bhaskar, K., Varadan, T.K., Ali, J.S.M., 1996. Thermoelastic solution for orthotropic and anisotropic composite laminates. Composites Part B: Engineering 27 (5), 415–420.

Birsan, M., 2009. Thermal stresses in cylindrical Cosserat elastic shells. European Journal of Mechanics - A/Solids 28 (1), 94–101.

Brischetto, S., 2009. Effect of the through-the-thickness temperature distribution on the response of layered and composite shells. International Journal of Applied Mechanics 1 (4), 1–25.

Brischetto, S., Carrera, E., 2009. Thermal stress analysis by refined multilayered composite shell theories. Journal of Thermal Stresses 32 (1), 165–186.

Brischetto, S., Leetsch, R., Carrera, E., Wallmersperger, T., Kröplin, B., 2008. Thermo-mechanical bending of functionally graded plates. Journal of Thermal Stresses 31 (3), 286–308.

Carrera, E., 1995. A class of two-dimensional theories for multilayered plates analysis, Accademia delle Scienze di Torino. Memorie Scienze Fisiche 19–20, 1–39.

Carrera, E., 2000. An assessment of mixed and classical theories for the thermal stress analysis of orthotropic multilayered plates. Journal of Thermal Stresses 23 (9), 797–831.

Carrera, E., 2002. Temperature profile influence on layered plates response considering classical and advanced theories. AIAA Journal 40 (9), 1885–1896.

Carrera, E., 2003. Theories and finite elements for multilayered plates and shells: a unified compact formulation with numerical assessments and benchmarking. Archives of Computational Methods in Engineering 10 (3), 215–296.

Khare, R.K., Kant, T., Garg, A.K., 2003. Closed-form thermo-mechanical solutions of higher-order theories of cross-ply laminated shallow shells. Composite Structures 59 (3), 313–340.

Khdeir, A.A., 1996. Thermoelastic analysis of cross-ply laminated circular cylindrical shells. International Journal of Solids and Structures 33 (27), 4007–4017.

Leissa, A.W., 1973. Vibration of Shells, NASA SP-288. National Aeronautics and Space Administration, Washington, USA.

Noor, A.K., Burton, W.S., 1992. Computational models for high-temperature multilayered composite plates and shells. Applied Mechanics Reviews 45 (10), 419–446.

Rolfes, R., Noack, J., Taeschner, M., 1999. High performance 3D-analysis of thermo-mechanically loaded composite structures. Composite Structures 46 (4), 367–379.

Thornton, E.A., 1996. Thermal Structures for Aerospace Applications, AIAA Education Series. AIAA, Reston, VA, USA.

Tungikar, V., Rao, B.K.M., 1994. Three dimensional exact solution of thermal stresses in rectangular composite laminates. Composite Structures 27 (4), 419–430.

Wu, Z., Chen, W., 2008. A global-local higher order theory for multilayered shells and the analysis of laminated cylindrical shell panels. Composite Structures 84 (4), 350–361.